Performance of the IEEE 802.15.4a access protocol under preamble-based clear channel assessment

Paúl Medina, Jaime Sánchez, José-Rosario Gallardo

Centro de Investigación Científica y de Educación Superior de Ensenada (CICESE)
Carretera Ensenada-Tijuana No. 3918, Zona Playitas, Ensenada, B. C. México. C.P. 22860
pmedina@cicese.mx, jasan@cicese.mx, gallardo@site.uottawa.ca

Abstract. This work reviews the clear channel assessment methods available for the different physical layer options of IEEE 802.15.4 networks, which are used by the CSMA-CA access algorithm at the MAC sublayer in order to determine the channel availability. Then it focuses on the preamble-based channel assessment mechanism, used exclusively by the Time Hopping Ultra Wide Band physical layer, and analyzes the effectiveness of this mechanism in reaching the ultimate goal of the access algorithm, which is to avoid frame collisions. Owing to the fact that preamble-based clear channel assessment require of searching preamble symbols, the paper goes deep into the preamble format and synchronization algorithms.

Keywords: IEEE 802.15.4a, Time Hopping Ultra Wide Band (TH-UWB), Clear Channel Assessment (CCA), preamble sensing, Energy Detection (ED).

1 Introduction

In a typical IEEE 802.15.4 network, the devices transmit frames to their coordinator node, which is in charge of organizing the communications with its children nodes, among other responsibilities. Two kinds of communications are distinguished: beacon-enabled and non-beacon-enabled [1]. In the beacon-enabled option, the coordinator periodically transmits a beacon frame, which serves as a reference to create a superframe structure. The first portion of the superframe is assigned for random access and uses the slotted CSMA-CA protocol. Optionally, the coordinator can create a contention-free access section and an inactivity period within the same superframe. In the non-beacon-enabled option, there is only a random access mode, controlled by the unslotted CSMA-CA protocol, whose operation is strongly linked to the carrier sense mechanism used to determine the channel availability, this mechanism is also known as Clear Channel Assessment (CCA) [2].

All of the physical layer options considered in the original IEEE 802.15.4 standard consist of some kind of continuous-wave modulation, for which it is relatively easy to determine the channel availability. The original standard specifies three different CCA-options that indicate a busy medium whenever: 1) the energy in the band is above a fixed threshold, 2) there is a signal in the band compliant with the specifications, and 3) the combination of the two previous options. In the standard,

Advances in Computer Science and Electronic Systems
Research in Computing Science 52, 2011, pp. 255-264

Received 23/01/11
Accepted 20/02/11
Final version 07/03/11

these options are named CCA-1, 2, and 3, respectively [1].

The IEEE 802.15.4a standard, released in 2007 [3] as an amendment to the original IEEE 802.15.4 specifications, adds two new options to the physical layer of these networks, one based on Chirp Spread Spectrum and another based on TH-UWB (Time Hopping Ultra Wide Band). With respect to the medium access control, the amendment keeps the same MAC sublayer but appends three new ways of CCA for the exclusive use of TH-UWB physical layer; namely CCA-4, 5, and 6. These new CCA options take into consideration the low duty cycle of TH-UWB signals, which hampers the common ways of performing the CCA in wireless environments.

In this work we study how these modifications in the CCA mechanism affect the performance of the MAC sublayer. Specifically, we are interested in investigating the performance of unslotted CSMA-CA protocol when the CCA-5 mechanism is used as the carrier-sense criterion at the physical layer. Important to mention that even though lot of research has been already done about the CCA and CSMA-CA, all of them rely on the continuous wave CCA. The originality of this work is to deal with the TH-UWB CCAs, which up to the authors' knowledge has not been explored yet.

The organization of the paper is as follows. Section 2 describes the preamble format of the IEEE 802.15.4a specifications, then Section 3 describes the new CCA-options which are based on this preamble format. Later, Section 4 studies a representative scenario evaluated trough simulations, and finally Section 5 concludes the document.

2 IEEE 802.15.4a preamble format

The IEEE 802.15.4a standard defines a physical layer based on pulses transmissions in the 0-10 GHz band. It specifies 16 FDM channels in this band, 12 of them are 500 MHz wide (-3dB bandwidth) and 4 of 1 GHz. The exact pulse shape is not defined, but it instead should fill some requirements in terms of the correlation with a reference pulse. For instance, in a 500 MHz channel the reference signal is a root raised cosine pulse with roll-off parameter $\beta = 0.6$ and 2 ns wide.

The preamble consists of N_{sync} repetitions of the preamble symbol S_i, where S_i is a sequence of pulses and blank spaces codified using a preamble code C_i. The standard specifies 8 preamble codes of 31 elements ($C_i, i = 1, 2, \ldots 8$), each of them consists of a sequence of ternary elements $c_{ij} \in \{-1, 0, 1\}$. These 8 codes were selected for its use in the preamble symbols of IR-UWB thanks to their properties of perfect autocorrelation in both coherent and non-coherent detection. They are also balanced sequences because all of them have almost the same amount of zero and non-zero elements (15 zero and 16 non-zero).

In Fig. 1a it is shown how a preamble symbol S_i is constructed from its corresponding preamble code C_i. It is observed that S_i constitutes an L length spreading of C_i, this means that after a pulse of polarity set by C_i (or the absence of the pulse in the case where $C_i(k) = 0$) there are inserted $L - 1$ empty chips. As an example the figure also shows a scheme of a preamble symbol of $L = 64$. Fig. 1b illustrates the synchronization header (SHR), which starts with a long sequence of repetitions of the preamble symbol and finishes with the start frame delimiter (SFD). The SFD is a predetermined sequence of full, inverted, or empty preamble symbols. Later, on Fig 1c, it is observed that after the SHR transmission follows the physical

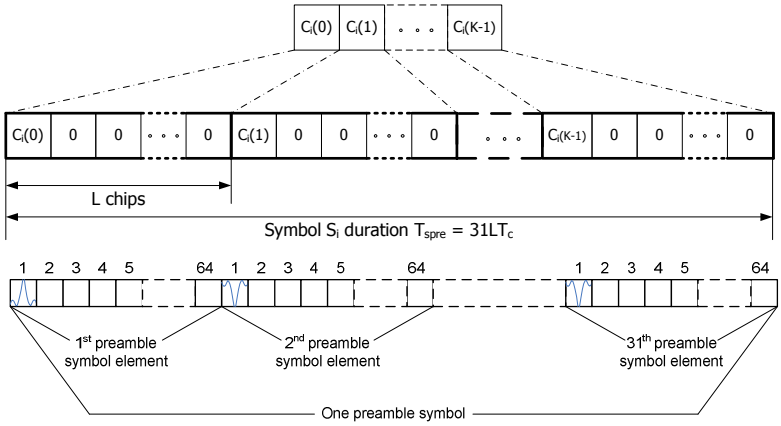

a) Structure of the preamble symbol

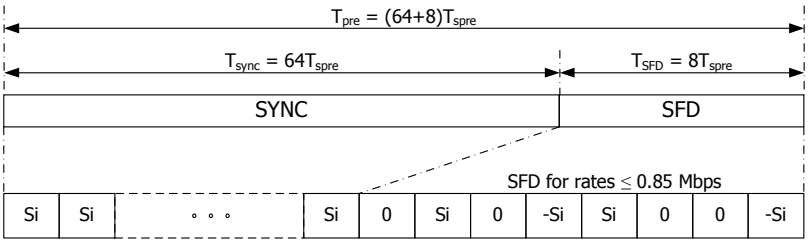

b) Preamble format

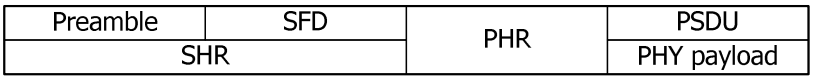

c) Physical layer frame format

Fig. 1. Preamble.

layer header (PHR) of 19 bits length, followed by the payload (PSDU) of 127 bytes maximum length.

Due to the scope of this work, the format of the data symbols is not shown; however it is important to highlight two of the key differences between the data and preamble symbols: 1) the preamble does not use a time-hopping sequence, then the pulse position is not randomized as in the data symbols; 2) in the data symbols the information is transmitted in pulses bursts, in the preamble symbol the pulses are transmitted isolated. It is also important to emphasize that all the nodes use the same time-hopping sequence in the data symbols and the same code in the preamble, so that the multiple access relies on the carrier sense, the signal low duty cycle, and the non-synchronism in the start of frame transmissions.

3 The new clear channel assessment (CCA) options

As was mentioned in Section 1, the CCA is a critical component of the unslotted CSMA-CA algorithm, used as the access protocol by IEEE 802.15.4 networks. Although some ways of performing the CCA has been stated in the original standard, the TH-UWB physical layer, because of its impulsive nature, is unable to follow them, and then it has to specify its own CCA-strategies. Continuing the numbered sequence the new standard enumerates the new CCA options as CCA-4, 5, and 6. In the following paragraphs is described how these options work.

CCA-4 option consists of always indicating the availability of the wireless channel, turning the CSMA-CA access into ALOHA. The CCA options 5 and 6 try to decrease the collision among frames through the use of preamble sensing. Both of them are based on the fact that preamble and data symbols follow a different modulation format [3], with preamble symbols being easier to detect than data symbols when the receiver is not synchronized to the time-hopping sequence. In this case, data symbols seem more like random noise than preamble symbols because of the random position of pulses within the data symbols given by the time-hopping sequence being used.

The CCA-5 method consists of indicating a busy channel upon detection of a preamble symbol, and it continues indicating a busy channel for T_{max} seconds after the last preamble symbol has been detected, where T_{max} is the time necessary for the transmission of a maximum-length frame plus its acknowledgment. T_{max} only depends on the transmission scheme and is always the same value even if maximum-length frames are never transmitted and MAC frame acknowledgments are never used (frame acknowledgment is optional in all access schemes of the standard). Fig. 2 shows just an example that illustrates the behavior of CCA-5.

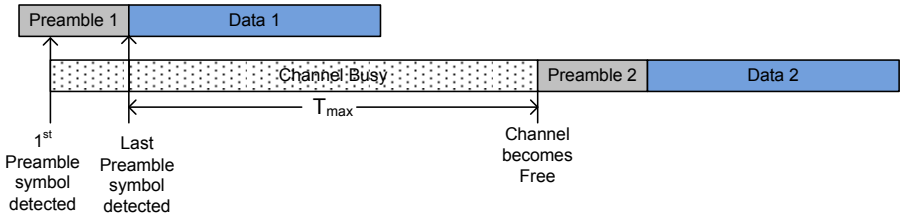

Fig. 2. CCA-5 operation example

The CCA-6 method, on the other hand, requires the insertion of preamble symbols in between the data symbols, enabling the neighbors to detect the current transmission in a similar way to that done by the continuous-carrier schemes. It is important to mention that the CCA-6 method is able to learn the channel availability without the long delays introduced by the CCA-5 method, at the cost of increasing the time required for a frame transmission.

In this work we study how these new CCA mechanisms affect the performance of the MAC sublayer. Specifically, we are interested in investigating the performance of unslotted CSMA-CA protocol when the CCA-5 mechanism is used as the carrier-sense criterion at the physical layer. Our interest in CCA-5 comes out because of, as a compensation of being unable to determine the channel availability immediately, it

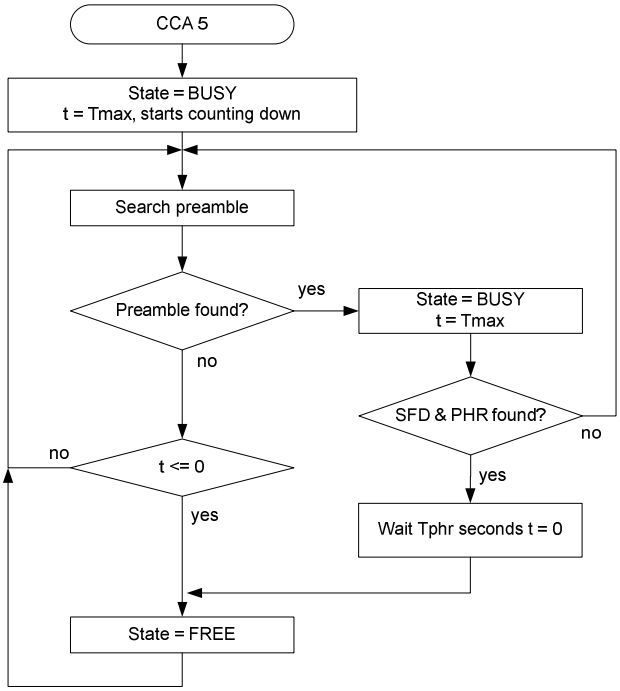

Fig. 3. CCA-5 Flowchart

has to introduce the use of a timer for the periods where it is not possible to perform a physical preamble sensing.

For a better understanding, Fig. 3 shows a flowchart of CCA-5 operation. When the MAC sublayer requests to the PHY layer to evaluate the medium availability with the CCA-5, it triggers the algorithm shown in Fig. 3, indicating a busy medium at the beginning and looking for preamble symbols over the air. It must pass T_{max} seconds without detecting any preamble symbol for changing the channel state to free. Once the channel is declared free it remains free until a preamble symbol is detected and then the state is changed to busy. Again it should pass T_{max} seconds with no preamble detected for the status to return back to free, and so on. It is observed in the flow chart that the T_{max} countdown can be shortened if the SFD is detected and the PHR is decoded. When that happens, the node can read the duration field contained in the PHR, so it can know when the frame will end and declare a free channel before T_{max} countdown concludes. This is known as 'virtual sensing' in IEEE 802.11 networks [5], however in TH-UWB it is done in the physical layer while in 802.11 it is performed at the MAC sublayer.

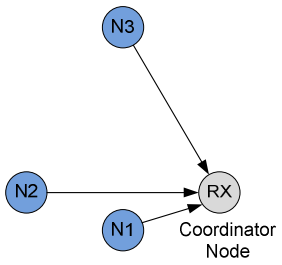

Relative link powers in dB

	N1	N2	N3	RX
N1	-	0	-3	0
N2	0	-	-3	-3
N3	-3	-3	-	-3
RX	0	-3	-3	-

Fig. 4. Scenario of study

4 Case of study and results

Fig. 4 shows the scenario considered for the performance study of the CCA-mechanisms. In such scenario there are one receptor node (RX) and three transmitter nodes (N1, N2, and N3). The traffic source of each transmitter node generates maximum length frames following a Poisson process with a rate of 100 frames/second. The transmitter nodes contend for the transmission of each frame following the access rules of unslotted CSMA-CA with the CCA-4 or 5. Observe that the distances between each pair of nodes are different and each link is received with different power. Fig. 4 also includes a table that shows the relative power in dB of each node link, where it is observed that:

- N1 signal reaches RX with more power (0 dB)
- N2 and N3 signals reach RX with the same power (-3 dB, the half of N1 signal)
- The power of link N1-N2 (0 dB) is higher than the link powers N1-N3 and N2-N3 (-3 dB both)
- Node RX could be seen as the coordinator node with which the children nodes (transmitters) have to communicate.

The scenario presented was evaluated through computer simulations in Matlab. It is considered that all the links use the data rate of 0.85 Mbps with a mean peak repetition frequency of 3.9 MHz, which means 4 pulses per data burst are used in the data symbol. For a detailed explanation about these parameters check [6]. Table 1 lists the main parameters used at the physical layer, where, for obvious reasons, is made emphasis in the preamble related parameters. The channel model used was the CM1 [7], which is an UWB channel model for indoors with line of sight.

At the receiver side, a non-coherent scheme based in energy detection is used, with an integration time of 8 ns [8]. The energy detector simply integrates over a period of time the square of the received signal. This scheme was adopted because of its simplicity, and also because it constitutes the most feasible low-cost scheme with the current technology. The synchronization method used was the one employed by [9] for this kind of reception, and the same synchronization parameters were also picked. Broadly speaking, in this method the energy samples are correlated with a binary mask constructed following the code preamble. The correlation samples are organized in vectors, where the number of elements in each of them corresponds to one preamble symbol. When the maximum value lies in the same position over several consecutive vectors the detection of a preamble symbol is declared. Later, only in the RX node, it is performed the fine synchronization algorithm, the looking for the start frame delimiter, the data and the Reed-Solomon decoding.

Figs. 5 and 6 show the main results of this research work for the explained scenario of study. For comparison purpose, both figures show at the left side the results when the CCA-5 is used as the channel sense mechanism, and in the right side the corresponding results when it is used the CCA-4, which means that the unslotted CSMA-CA access turns to ALOHA.

The figure of merit sketched in Fig. 5 is the Overlapping Frame Rate (OFR) per node, obtained for each transmitter node as the number of overlapped frames divided into the total transmitted frames:

$$\mathrm{OFR(node\ i)} = \frac{\textit{Overlapped Frames}(\mathrm{node\ i})}{\textit{Total Transmitted Frames}(\mathrm{node\ i})} \qquad (1)$$

Observe that we preferred the word 'Overlap' instead of 'Collision', due that as we will see later not all the frame overlaps turn into a destructive collision, as happens in the continuous wave transmission. Turning back our attention to Fig. 5a, we can see how the effectiveness of the CCA-5 in avoiding the frame overlap is proportional to the SNR with whom the pulses of the potential interferer are detected. It is also seen

Table 1. Physical layer specifications.

Data rate	0.85 Mbps
Chip Period (Tc)	2 ns
Data Symbol Length	512 chip periods
Preamble code spreading (L)	64 chips
Preamble length	64 preamble symbols
SFD length	8 preamble symbols
Preamble code number	5th in all nodes
Channel model	CM1 [7]
Tmax	1.72 ms
Reed-Solomon decoding	yes
Receptor	Based on Energy Detection
Integration Time (Tint)	8 ns (4 chips)

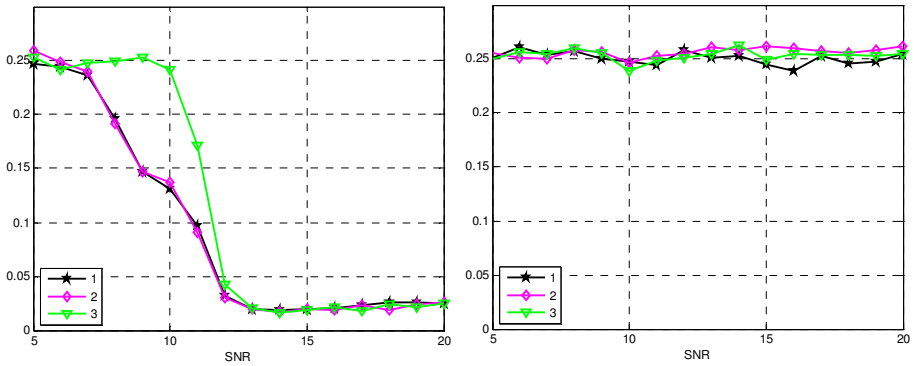

a) Unslotted CSMA with CCA-5 **b)** Unslotted CSMA with CCA-4 = ALOHA

Fig. 5. Overlapping Frame Rate: Number of overlapped divided by total of transmitted frames, per node.

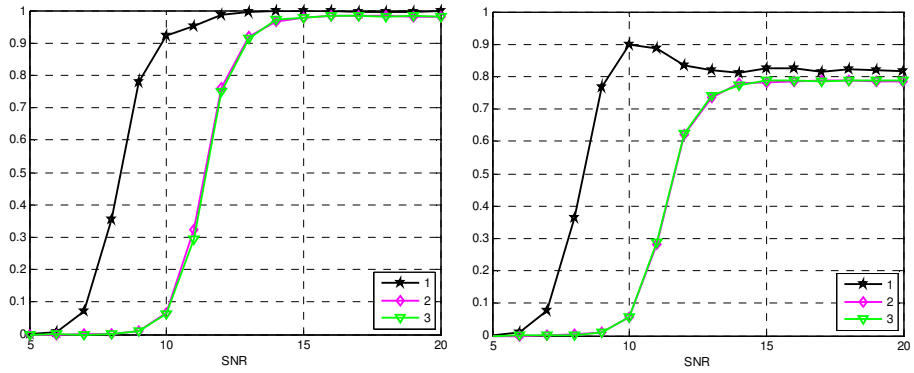

a) Unslotted CSMA with CCA-5 **b)** Unslotted CSMA with CCA-4 = ALOHA

Fig. 6. Successful synchronization rate in the node RX: Number of frames successfully synchronized divided by the total of transmitted frames, per node.

that transmitters N1 and N2 are more efficient in avoiding the frame overlap since the link N1-N2 is shorter than the links between these nodes and N3, then N3 requires higher SNR in order to reduce the overlapping. A floor level is observed in the overlapping, that comes from the vulnerability period of the CCA-5 in which it is impossible to detect a transmission that just begun.

Fig. 5b only confirms that in the CCA-4 nothing is done for avoid the overlapping (ALOHA), in fact they remains at the same level matter neither the SNR nor the node position. It is well-known that this level only depends on the network load and the frame size [10]. Notice as well that, when the SNR is not higher enough the CCA-5 cannot detect the current transmissions and has a similar behavior to CCA-4.

Fig. 6 sketches the Successful Synchronization Rate (SSR) for each node, obtained in the RX for each transmitting node making the following division:

$$\mathrm{SSR}(\text{node i}) = \frac{\textit{Successfull Syncronized Frames}(\text{node i})}{\textit{Total Transmitted Frames}(\text{node i})} \qquad (2)$$

It can be seen in Fig. 6 that, in both CCA schemes, node N1 gets a higher synchronization probability because of it is closer to the RX node than N2 and N3, and those nodes have exactly the same trend because their links to RX have exactly the same distance. As we previously mentioned, in Fig. 6a can be observed that not all overlapping is destructive, because the synchronization efficiency is close to one; even though, as seen in Fig. 5a, overlapping is not completely eliminated by CCA-5. Fig. 6a shows that CCA-4 cannot reach the synchronization rate achieved by CCA-5. Again, the level shown is surely dependent on the network load.

It is noticeable that the figures of merit are both dependent on the received signal strength, however the overlapping is dependent on how transmitter 'hears' to the nodes it is contending with, and synchronization depends in how the intended receiver 'hears' the transmitter.

5 Conclusions

The performance of the access protocol with the CCA-5 is evaluated and compared to that in which the CCA-4 is used (i.e. no carrier sense), both when energy detection receivers are employed. As expected, the use of CCA-5 brings a better performance to the access protocol, which can be seen in the plots of overlapping and synchronization rates against SNR (signal-to-noise ratio) achieved by each channel assessment method.

The effectiveness on CCA-5 in the avoidance of frame collision was found superior to CCA-4, however the level of implementation penalties introduced at the physical layer have not yet been analyzed. It was observed in both schemes a kind of capture effect, where in overlapped transmissions the receptor synchronizes with one of the frames. Just like in phase modulation of continuous carrier, in TH-UWB the receiver also tends to synchronize with the strongest signal. However, unlike the narrowband schemes, in TH-UWB if the receiver is already synchronized to a weak signal it will never synchronize to a stronger signal that comes after.

At this point of our research we made our discussion based on the results obtained by computer simulations of different network scenarios. A mathematical analysis that gives us a better understanding of the system behavior is our next step in the research path.

References

1. IEEE 802.15.4-2006. "Wireless Medium Access Control (MAC) and Physical Layer (PHY) Specifications for Low-Rate Wireless Personal Area Networks (LR-WPANs)." IEEE Standard 802.15.4, 2006 Edition.

2. I. Ramachandran, S. Roy, "Clear Channel Assessment in Energy-constrained Wideband Wireless Networks," IEEE Wireless Communications Magazine, 2007, Vol. 14, No.
3. IEEE 802.15.4a-2007. "Wireless Medium Access Control (MAC) and Physical Layer (PHY) Specifications for Low-Rate Wireless Personal Area Networks (LR-WPANs). Amendment 1: Add alternate PHYs." IEEE Standard 802.15.4a, 2007 Edition.
4. F. A. Molish, P. Orlik, Z. Sahinoglu, J. Zhang, "UWB-based sensor networks and the IEEE 802.15.4a standard – a tutorial," First International Conference on Communications and Networking in China, 2006 (ChinaCom '06).
5. Gast, M. 2002. "802.11 Wireless Networks: The Definitive Guide". O´Reilly. First Ed. Sebastopol, California.
6. P. Medina, J. R. Gallardo, J. Sánchez, F. Ramírez Mireles, "Impact of Delay Spread on IEEE 802.15.4a Networks with Energy Detection Receivers", Journal of Applied Research and Technology, Vol. 8, No. 3., 2011.
7. Molish F. A., Balakrishnan K., Cassioli D., Chong C., Emami S., Fort A., Karedal J., Kunisch J., Schantz H., Schuster U. & Siwiak K., "IEEE 802.15.4a channel model – final report," 2004.
8. H. Urkowitz, "Energy detection of unknown deterministic signals," Proc. of IEEE, vol. 55, pp. 523-531, Abril 1967.
9. M. Flury, R. Merz, J.-Y. Le Boudec & J. Zory, Performance Evaluation of an IEEE 802.15.4a Physical Layer with Energy Detection and Multi-User Interference, IEEE International Conference on Ultra-Wideband (ICUWB 2007), September 2007.
10. N. Abramson, "Development of the AlohaNet," IEEE Trans. Info. Theory, vol. IT-31, no. 2, Mar. 1985, pp. 119–23